Australian Journal of Earth Sciences (2000) **47**, 1065–1076

Evidence for Palaeozoic magmatism recorded in the Late Neoproterozoic Marlborough ophiolite, New England Fold Belt, central Queensland*

M. C. BRUCE AND Y. NIU

Department of Earth Sciences, University of Queensland, Qld 4072, Australia.

The ultramafic–mafic complex in the Marlborough terrane of the northern New England Fold Belt is dominated by members of a Neoproterozoic (*ca* 560 Ma) ophiolite (V1). The ophiolite has been intruded by the products of three Palaeozoic tectonomagmatic episodes (V2, V3 and V4). The V2 magmatic episode is represented by tholeiitic and calc-alkaline basalts and gabbros of island-arc affinities. Sm/Nd isotopes give a whole-rock isochron age of 380 ± 19 Ma (2σ) to this episode, some 180 million years younger than the V1 ophiolitic rocks. The V3 magmatic episode includes tholeiitic and alkali basalts with enriched geochemical signatures characteristic of intraplate volcanism. A whole-rock Sm/Nd isochron age of 293 ± 35 Ma is obtained for this event. A fourth magmatic event (V4) is represented by basaltic andesites and siliceous intrusives with geochemical features similar to modern adakites. This event has its type locality in the Percy Isles. These data provide tectonic and geochronological constraints for the previously enigmatic Marlborough terrane and as such contribute to the ever-evolving understanding of New England Fold Belt development.

KEY WORDS: Marlborough terrane, Neoproterozoic, ophiolite, Palaeozoic, tectonics.

INTRODUCTION

The New England Fold Belt refers to the easternmost part of the Tasman Orogenic Zone of eastern Australia, a zone which constitutes a segment of a much larger orogenic system that developed along the Pacific margin of Gondwana (Coney *et al*. 1990). The fold belt is a tectonic collage of numerous terranes comprising subduction/accretion units and extensional basins overprinted by convergent structures of the Hunter–Bowen Orogeny (Leitch 1974, 1975). Numerous tectonic models have been proposed for the development of the New England Fold Belt (Day *et al*. 1978; Cawood & Leitch 1985; Murray *et al*. 1987; Henderson *et al*. 1993; Holcombe *et al*. 1997; to name but a few). However, there are apparent inconsistencies among many of these models (Flood 1988). The major hurdle against a unified tectonic model(s) for the New England Fold Belt results from the lack of understanding/knowledge of the tectonic setting and geochronology of rocks from individual terranes. We have undertaken a broad study into one such terrane, the Marlborough terrane, which until now very little was known, despite its potential significance in New England Fold Belt development (Murray 1974).

The Marlborough terrane is located within the northern segment of the New England Fold Belt (Figure 1) and contains an ultramafic–mafic complex dominated by remnants of a Neoproterozoic oceanic basin (Bruce *et al*. 2000). These lithologies are among some of the oldest rocks thus far identified throughout the New England Fold Belt and as such provide us with a prime opportunity to reveal the pre-Palaeozoic history of the fold belt.

Detailed petrological, geochemical and geochronological data of rocks from the Marlborough ultramafic–mafic association have revealed four tectonomagmatic events which from oldest to youngest are: V1, formation of the ophiolite substrate; V2, emplacement of a mafic suite of tholeiitic and calc-alkaline intrusives; V3, intrusion of tholeiitic and alkaline dykes; and V4, emplacement of suites of differentiated calc-alkaline granitoids. The V1 event has been discussed elsewhere (Bruce *et al*. 2000). In this paper we outline the post-ophiolitic Palaeozoic events (V2–V4) and discuss the tectonic implications for V2 and V3 magmatism.

PETROLOGY OF V2, V3 AND V4 ROCKS

The post-ophiolitic magmatic rocks can be divided into tholeiitic, calc-alkaline and alkaline affinities.

V2 intrusive rocks

THOLEIITE

Tholeiitic basalt occurs as dykes and fault-bounded blocks in the ophiolite (V1) sequence. The dykes either intrude the sequence or are thrust-emplaced along with serpentinite. In hand specimens, the tholeiitic metabasalt/dolerite rocks are dark-grey and range from an equigranular to a

*A fuller version of Table 1 is a Supplementary Paper lodged with the National Library of Australia (Manuscript Section); copies may be obtained from the Business Manager, Geological Society of Australia.

plagioclase-phyric texture. They are invariably metamorphosed to greenschist facies and are composed mainly of small (< 1 mm) glossy black, elongated amphibole crystals set in a fine-grained, greyish-white feldspar matrix. Porphyritic metadolerites display a similar mineralogy, but contain large tabular to anhedral, greenish-white feldspar phenocrysts up to 6–7 mm in some samples.

In thin-section, relict igneous olivine, clinopyroxene (augite to salite in composition) and magnetite/ilmenite are observed and are overprinted by a metamorphic assemblage of hornblende + actinolite + albite + chlorite ± prehnite/pumpellyite ± epidote ± carbonate ± sphene. Hydrogrossular appears in some metasomatised samples. The plagioclase phenocrysts in the porphyritic dolerites have been totally altered to chlorite and sericite assemblages.

CALC-ALKALINE MAGMATISM

Calc-alkaline rocks occur as gabbroic intrusions and fine-grained doleritic dykes cross-cutting and in structural contact with serpentinite. The dykes range from seriate textured to equigranular with plagioclase of andesine ($An_{34–41}$) composition and clinopyroxene partially altered and overprinted by a metamorphic assemblage of hornblende + actinolite + chlorite ± prehnite/pumpellyite ± epidote ± sphene. Igneous magnetite relicts are observed in some samples. The gabbros are commonly coarse grained (up to 6 mm) with relict augite and hornblende crystals displaying intergranular texture with 0.5–1 mm tabular, partially saussuritised andesine crystals and minor metamorphic actinolite and prehnite. A finer grained gabbro dominated by a metamorphic assemblage of hornblende + actinolite + plagioclase + chlorite + epidote also occurs. Relict chromium spinel crystals in the gabbro have Cr# [Cr/(Cr + Al)] = 0.68–0.80, typical of spinels in volcanic-arc rocks (i.e. Cr# > 0.60; Dick & Bullen 1984).

V3 intrusive rocks

Metamorphosed alkaline and tholeiitic dolerite dykes also intrude the ophiolite sequence (V1). In hand specimen, the alkaline dykes are relatively fine grained and equigranular in texture. They consist of black elongated to tabular amphibole crystals in a matrix of anhedral chlorite/hornblende and plagioclase. V3 dykes are commonly cross-cut by carbonate veins. In thin-section, the dykes display relict igneous clinopyroxene and magnetite overprinted by secondary prismatic, equant and lath-like hornblende crystals, fibrous actinolite, tremolite and albite in a feldspar–quartz mesostasis groundmass. Magnetite is ubiquitous but commonly rimmed by ilmenite. The tholeiitic dykes have a similar mineralogy to the alkaline dykes with the major difference being the presence of relict olivine crystals in the former.

V4 intrusive rocks

Basaltic andesite dykes intrude the serpentinite of the V1 event. These dykes are metamorphosed and their igneous

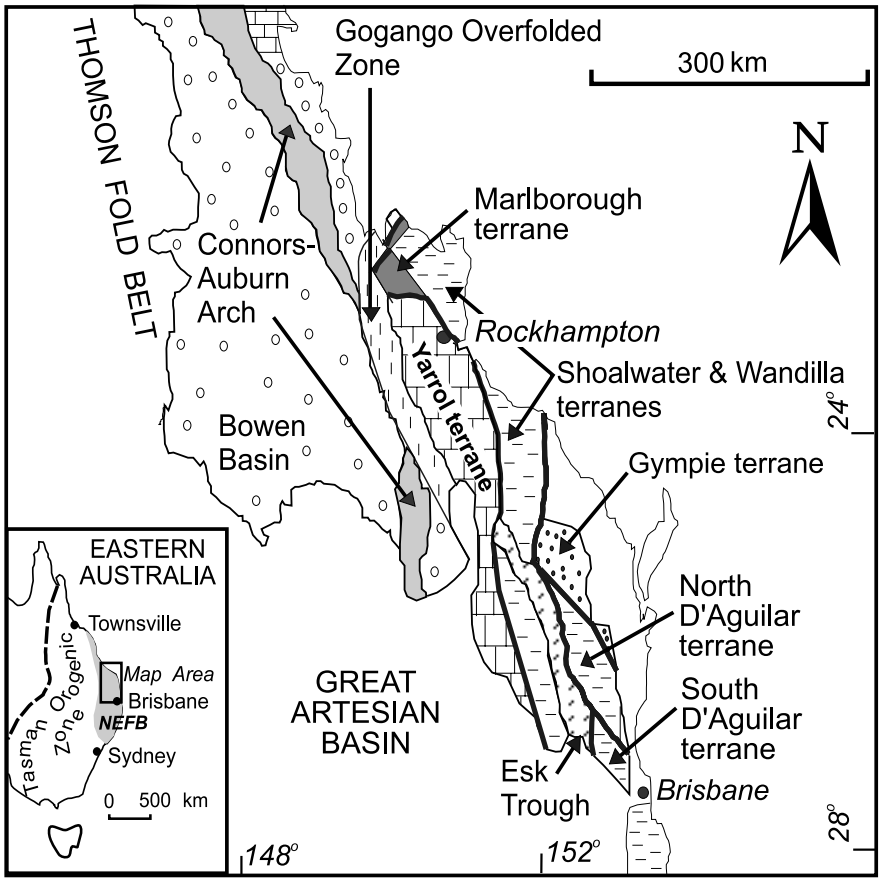

Figure 1 Simplified geological map of the northern New England Fold Belt showing the location of the Marlborough terrane. Inset indicates location of map area within the New England Fold Belt (NEFB), which is the easternmost tectonic unit of the Tasman Orogenic Zone of eastern Australia.

mineralogy has been replaced by lath-like fibrous actinolite crystals embedded in a matrix of albite and chlorite with minor tremolite and secondary quartz. Diorite intrusions are in fault contact with the V1 serpentinite. The diorite displays intergranular textures, comprising primary hornblende and clinopyroxene crystals partially overprinted by an actinolite/hornblende + albite metamorphic assemblage. Locally plagioclase crystals are completely altered to chlorite. Relict chromium spinel is also present with Cr/Cr + Al = 0.56–0.60, but has been largely altered to 'ferro' chrome compositions.

Trondhjemite and tonalite dykes locally intrude the magmatic products of the V1 and V3 rocks. The trondhjemite is a medium-grained rock with a primary mineralogy of quartz and plagioclase, overprinted by a predominantly chlorite and sericite metamorphic assemblage. The tonalite has a similar mineralogy with less quartz and more plagioclase plus overprinting fibrous Mg-rich actino-

Table 1 Major and trace-element concentrations of magmatic rocks from the V2, V3 and V4 tectonomagmatic events.

	V2 magmatism			V3 magmatism		V4 magmatism		
	MB5 Dolerite	MB96 Gabbro	MB112 Dolerite	MB38 Dolerite	MB62 Dolerite	MB20 Trondhjemite (adakite)	MB53 Basaltic andesite	MB57 Tonalite (adakite)
SiO_2	50.12	46.50	45.13	42.56	48.72	75.40	54.12	68.45
TiO_2	1.65	0.65	1.70	3.81	2.06	0.10	0.69	0.16
Al_2O_3	13.90	18.84	16.97	12.98	15.31	14.92	14.60	19.13
Fe_2O_3*	13.43	9.51	13.54	16.10	13.16	0.63	7.15	0.20
MnO	0.22	0.22	0.20	0.24	0.24	0.01	0.15	0.00
MgO	6.28	8.77	4.51	10.06	5.20	0.58	7.74	0.37
CaO	9.54	13.97	15.51	7.29	9.43	1.25	9.29	0.86
Na_2O	3.97	1.20	2.17	1.93	5.81	7.17	4.92	10.21
K_2O	0.16	0.11	0.24	0.51	0.18	0.28	0.19	0.15
P_2O_5	0.14	0.14	0.26	0.37	0.41	0.01	0.09	0.02
LOI	1.02	1.29	0.52	4.90	0.75	0.30	0.69	0.34
Total	100.43	101.18	100.74	100.75	101.25	100.65	99.62	99.90
Li	12.44	1.42	9.50	35.88	2.33	11.39	8.00	0.05
Be	0.38	0.45	0.38	1.27	0.46	0.44	0.64	0.74
Sc	42.67	24.88	40.88	38.45	32.16	0.72	25.52	18.31
V	375	192	455	354	244	6.98	171	0.07
Cr	82.49	240	18.37	62.81	16.33	68.96	263	2.54
Co	40.21	33.22	39.90	45.11	34.73	2.16	36.52	0.61
Ni	40.07	56.27	39.49	22.06	23.79	10.81	76.52	38.44
Cu	72.30	36.12	12.28	48.19	57.31	3.50	8.15	2.66
Zn	87.77	54.25	76.99	131	86.04	6.53	95.18	1.17
Ga	16.10	15.38	18.24	16.73	13.56	14.42	15.86	15.49
Rb	1.48	0.35	1.70	12.07	2.04	3.33	2.46	2.02
Sr	223	575	309	442	338	379	381	173
Y	28.60	10.79	26.41	50.68	25.74	1.09	17.44	1.21
Zr	73.41	24.66	42.52	249	67.92	57.56	53	16.13
Nb	1.46	0.76	1.03	7.97	7.86	1.18	2.29	1.37
Cs	0.16	0.03	1.06	1.16	0.07	0.83	0.16	0.03
Ba	50.75	22.14	172	248	124	146.40	63.41	148
La	3.83	3.70	4.62	12.60	10.47	13.56	6.07	33.19
Ce	11.20	9.24	12.68	33.92	24.65	25.96	14.71	58.64
Pr	1.94	1.40	2.10	5.23	3.67	2.76	2.17	6.07
Nd	9.79	6.64	10.66	25	16.69	9.04	9.22	18.83
Sm	3.42	1.84	3.44	7.19	4.51	1.48	2.52	2.30
Eu	1.18	0.69	1.46	2.40	1.92	0.41	1.00	0.27
Tb	0.75	2.05	4.41	9.02	0.80	0.08	3.09	0.08
Gd	4.58	0.33	0.78	1.54	5.39	0.86	0.49	1.01
Dy	5.13	2.15	5.15	10.10	4.96	0.29	2.91	0.27
Ho	1.07	0.45	1.10	2.10	0.98	0.04	0.65	0.05
Er	3.32	1.29	3.13	5.85	2.90	0.09	1.94	0.16
Tm	0.46	0.20	0.47	0.86	0.36	0.013	0.25	0.013
Yb	3.03	1.25	2.87	5.30	2.28	0.09	1.83	0.072
Lu	0.44	0.19	0.43	0.80	0.32	0.014	0.27	0.013
Hf	2.15	0.88	1.63	6.56	1.88	1.47	1.68	0.74
Ta	0.10	0.05	0.08	0.59	0.48	0.051	0.20	0.062
Pb	0.50	3.16	5.65	3.52	0.60	0.92	16.14	0.82
Th	0.40	0.62	0.46	1.82	0.83	2.96	2.27	5.26
U	0.13	0.22	0.14	0.50	0.25	0.20	0.45	0.19

Fe_2O_3* = total iron; concentration of trace elements in ppm.

lite and tremolite. These lithologies are variably affected by sodium metasomatism culminating in the occurrence of dykes that are largely composed of albite and quartz.

GEOCHEMISTRY

Analytical techniques

Analyses of representative samples are presented in Table 1 (the locations of all samples mentioned in the tables are given in Appendix 1). Samples for major element analyses were crushed in a TEMA tungsten-carbide mill. Major elements were determined using a Varian Liberty 200 Inductively Coupled Plasma–Atomic Emission Spectrometer (ICP–AES) at Queensland University of Technology, following the procedure of Kwiecien (1990). Precision (1σ) for most elements based on USGS standards (BCR-1, BIR-1, AGV-1 and G-2) is < 1.0%, and is < 2.0% for TiO_2 and P_2O_5.

For trace-element analyses, fine-grained samples were crushed in a soft-steel percussion mill and sieved down to a size of 500 μm. Grains were preferred to powders in order to minimise contamination from the TEMA mill and subsequent handling associated with the latter. The coarser plutonic samples were powdered in a TEMA chromium-steel mill to enable a representative portion of the bulk rock to be analysed. Trace elements were analysed on a Fisons VG Plasma Quad 2 Inductively-coupled Mass Spectrometer (ICP-MS) at the University of Queensland. Sample preparation follows the procedure described by Bruce *et al.* (2000).

Alteration

Many elements are susceptible to alteration during low-grade metamorphism (Cann 1969; Pearce 1976). This is particularly true for the alkali elements (e.g. Li, Na, K, Rb and Cs) and other large ion lithophile elements (LILE: Sr, Ba, Pb, U: Jochum & Verma 1996). In contrast, the high field strength elements (HFSE: such as Ti, Nb, Ta, Zr, Hf) and the rare-earth elements (REE: La, Ce, Pr, Nd, Sm, Eu, Gd, Tb, Dy, Ho, Er, Tm, Yb, Lu plus Y) are generally considered immobile (Campbell *et al.* 1984), except for a few light REEs (LREE) which may be mobile under conditions of high water/rock ratios and during carbonate alteration (Humphris 1984). As the mafic and intermediate rocks of the V2, V3 and V4 events of the Marlborough terrane have been metamorphosed to greenschist facies assemblages, our interpretation is thus focused primarily on the immobile HFSEs and REEs.

RESULTS

V2 INTRUSIVE ROCKS

The significant linear correlations between SiO_2 and FeO*/MgO defined by V2 rocks (Figure 2) can be readily

Table 2 Comparative major element data for rocks of the Marlborough terrane and southwest Pacific island-arc suites.

	Tholeiitic basalts		Basaltic andesites	
	Marlborough (V2)	Niua Fo'ou, Tonga SW Pacific	Marlborough calc-alkaline (V4)	Average SW Pacific calc-alkaline
	$n = 6$	$n = 5$	$n = 2$	$n = 176$
SiO_2	49.9 ± 1.1	49.8	54.0 ± 0.8	54.49
TiO_2	1.4 ± 0.2	1.5	0.7 ± 0.03	0.76
Al_2O_3	14.8 ± 0.8	14.8	15.0 ± 0.4	17.00
FeO*	10.6 ± 0.9	10.8	7.0 ± 0.7	8.37
MnO	0.2 ± 0.02	0.2	0.1 ± 0.02	0.16
MgO	5.9 ± 0.5	6.9	8.5 ± 1.1	5.18
CaO	10.2 ± 1.9	11.6	8.9 ± 0.6	9.10
Na_2O	5.1 ± 1.7	3.2	5.0 ± 0.1	2.98
K_2O	0.6 ± 0.7	0.2	0.2 ± 0.05	1.15
P_2O_5	0.18 ± 0.05	0.1	0.1 ± 0.01	0.22

Data from Niua Fo'ou Island after Ewart *et al.* (1977); average southwest Pacific calc-alkaline basaltic andesite after Ewart (1982). Data from Marlborough terrane (this study) are averaged data with 1σ. FeO* = total iron reported as FeO.

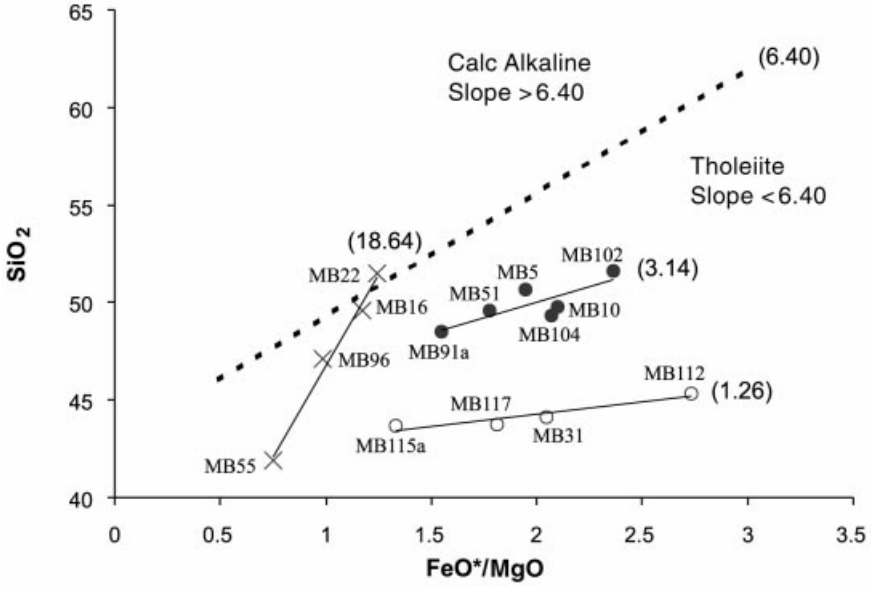

Figure 2 Rocks from the V2 intrusives of the Marlborough ophiolite (V1) divided into calc-alkaline and tholeiitic suites. Dotted line marks the slope discriminating between calc-alkaline and tholeiite trends (Miyashiro 1974). These divisions are also supported by REE patterns (Figure 3). Slopes of individual Marlborough series are markedly different and symbols denote individual series. Refer to Table 1 for sample numbers. FeO* = total iron reported as FeO.

explained by fractional crystallisation. This also suggests that metamorphism has not affected these elements significantly. Using the classification scheme of Miyashiro (1974) mafic rocks of the V2 event can be divided into two tholeiitic suites and one calc-alkaline suite based on their differentiation trends. Table 2 compares the basalts from

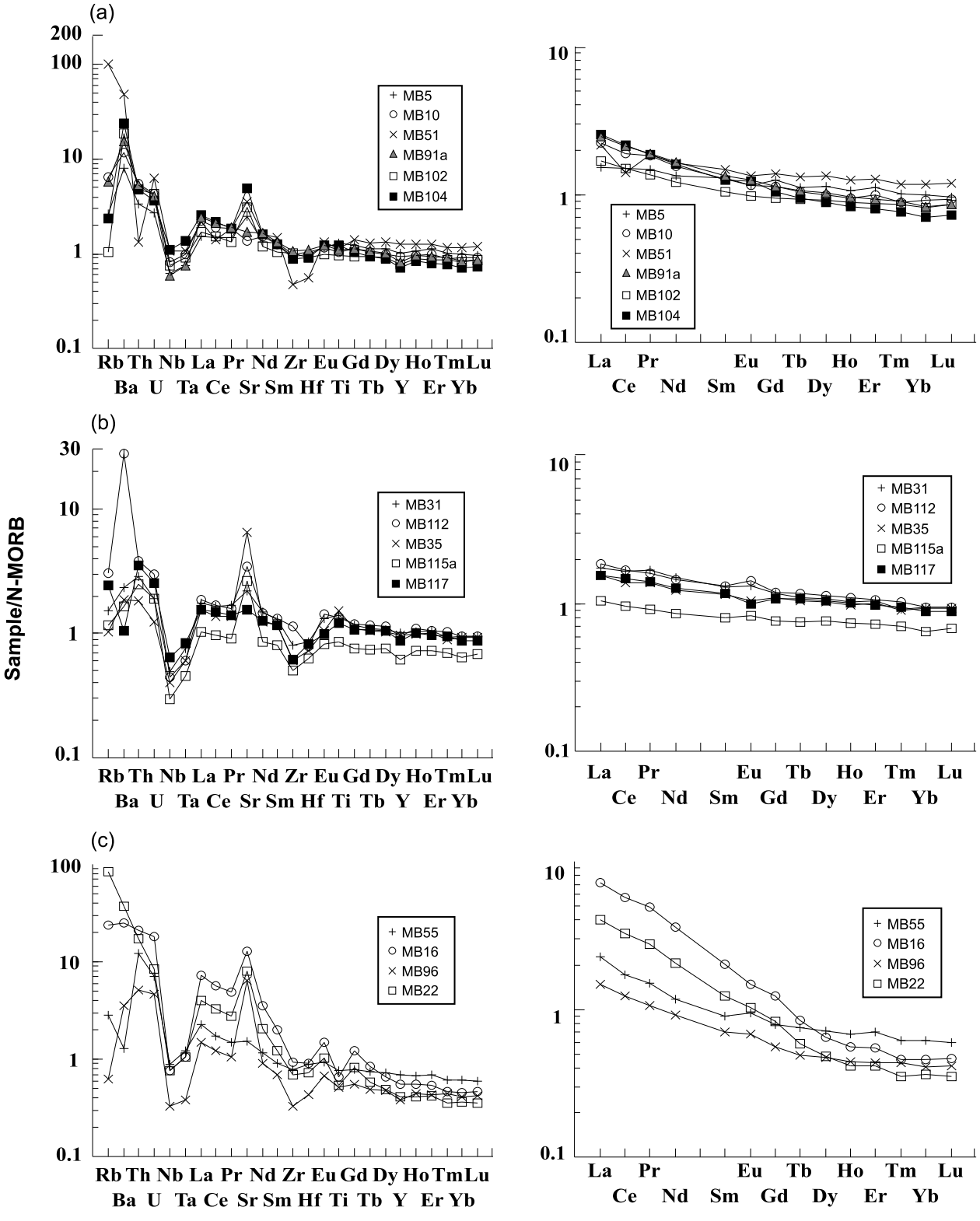

Figure 3 N-MORB-normalised incompatible multi-element (left) and REE diagrams (right) of the V2 magmatic rocks. Note the negative Nb–Ta anomalies and LREE enrichment, which are characteristic of arc lithologies (see text). Samples are grouped into three volcanic suites: (a) tholeiite suite I, (b) tholeiite suite II, (c) calc-alkaline suite I, based on fractionation trends (Figure 2) and REE patterns.

this event with the average island-arc basalts from the northern Tongan Islands (Ewart *et al*. 1977). The V2 tholeiitic basalts are very similar in composition to the high-Ti and low-Al island arc tholeiitic basalts of Niua Fo'ou, northern Tonga. The only appreciable difference is a higher Na_2O and K_2O concentration in the V2 tholeiitic basalts, which probably resulted from alteration/metamorphism.

Plots of trace elements normalised to the average N-MORB (Sun & McDonough 1989) are shown in Figure 3. The tholeiitic suites have high Th and low HFSE (Nb, Ta, Zr and Hf) contents relative to MORB, a feature characteristic of island-arc basalts (Pearce 1982). Enriched LILEs [Ba, Sr, Pb (not shown)] relative to MORB are also present as expected for arc rocks, but this could partly be due to metamorphism. However, slight enrichment in the LREE [Figure 3: $(Sm/Nd)_{N\text{-}MORB} = 0.78–0.97$] may suggest that the high Ba and Sr relative abundances may be primary, typical of arc lavas rich in LILE and LREE (Saunders & Tarney 1979; Perfit *et al*. 1980). The tholeiites plot in the field of volcanic-arc rocks on the Th–Hf–Ta discrimination diagram of Wood (1980) (Figure 4) and have elevated Hf/Th ratios (> 3), typical of island-arc tholeiites. Similarly, the calc-alkaline rocks are enriched in Th, Ba and Sr and depleted in Nb, Ta, Zr, Hf and Ti relative to MORB. The basalt–diorite–gabbro suite has high Sr/Nd, Ba/Nb and Th/Yb ratios. This, together with low Nb/La, Ti/V and LREE enrichment [$(Sm/Nd)_{N\text{-}MORB} = 0.56$] is consistent with the addition of a LREE- and LILE-rich aqueous fluid phase from a subducting slab to the overlying mantle wedge source (Perfit *et al*. 1980). All calc-alkaline rocks plot in the volcanic-arc field on the Th–Hf–Ta discrimination diagram and have low Hf/Th ratios (< 3), typical of calc-alkaline volcanics.

V3 INTRUSIVE ROCKS

CIPW norms suggest both alkali (nepheline–olivine normative) and olivine tholeiitic (hypersthene–olivine normative) basaltic dykes are present in this sequence. As many of the major and minor elements have been apparently mobilised, the CIPW results could be suspect. However, immobile trace-element distributions support the interpretations of normative reconstructions (see below). The low SiO_2 (< 45%) and high TiO_2 (4%) and Fe_2O_3* (16.2%) content of the olivine tholeiite is consistent with the petrographic observation of Fe–Ti oxide accumulation. Primitive-mantle normalised incompatible-element abundances display enriched signatures relative to the average N-MORB of Sun and McDonough (1989) (Figure 5). The alkali basalts have characteristically low Zr/Nb ratios (< 10) similar to oceanic-island basalts and E-type MORB (Sun & McDonough 1989). Negative Zr and Hf anomalies occur in the alkali basalts whereas a positive Zr and Hf anomaly is observed in the tholeiite. The Zr–Hf negative anomalies correspond with positive Eu anomalies whereas the negative Zr–Hf anomaly coincides with a positive Eu spike (Figure 5). This relationship could be interpreted as resulting from modal plagioclase variation, but this is not obvious petrographically. An alternative explanation for the Zr–Hf negative anomalies may be incomplete digestion of zircon crystals during sample preparation or zircon or

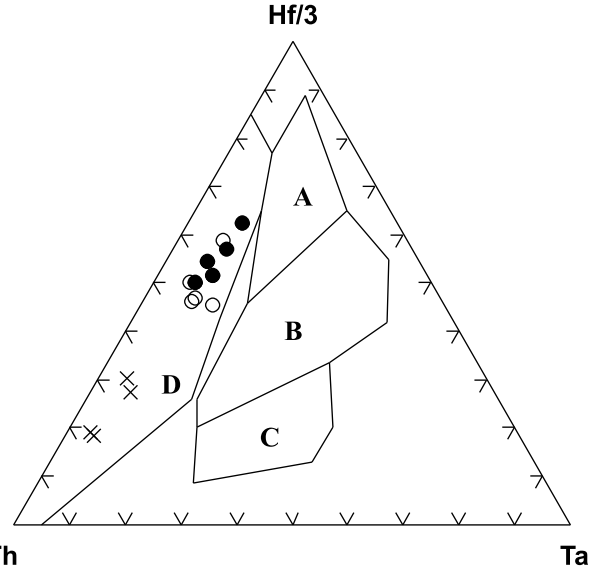

Figure 4 Th–Hf–Ta discrimination diagram of Wood (1980). A, N-MORB; B, E-MORB and within-plate tholeiites and differentiates; C, within-plate basalts and differentiates; D, destructive plate basalts and differentiates. Samples from the V2 event plot in the volcanic-arc field with the tholeiites having Hf/Th ratios > 3 and the calc-alkaline basalts Hf/Th ratios < 3. ●, tholeiite suite 1; ○, tholeiite suite 2; ×, calc-alkaline suite 1.

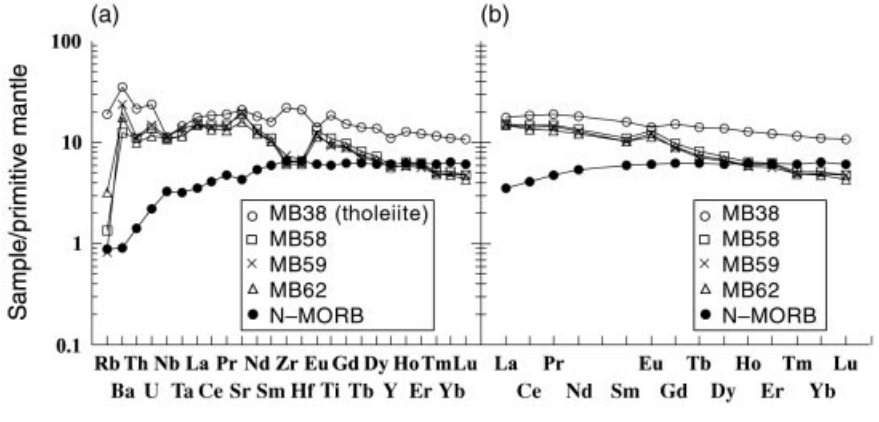

Figure 5 (a) Multi-element and (b) REE diagrams of basaltic rocks from the V3 event normalised to primitive-mantle values. Note the enrichment of incompatible elements compared to the average N-MORB (after Sun & McDonough 1989).

baddeleyite fractionation (Niu & Hékinian 1997). The tholeiite displays a slight Nb–Ta trough (Figure 5), which together with enrichment in Ba, Th, U, Sr, Zr and Hf may suggest contamination by continental crust (Cox & Hawkesworth 1985), although general enrichment in all incompatible elements may simply reflect the heterogeneity of the enriched mantle source. The basalts plot in the within-plate basalt field on the Zr–Y–Ti diagram of Pearce and Cann (1973) (Figure 6a) and in the continental flood-basalt field on the Ti–V diagram of Shervais (1982) (Figure 6b) with the exception of the Ti-rich tholeiite. Similarly, on the La–Y–Nb discrimination diagram of Cabanis and Lecolle (1989) (Figure 6c), the basalts overlap the field of continental basalts. However, on the Th–Hf–Ta diagram of Wood (1980) (Figure 6d), the alkali basalts plot in the field of E-MORB and within-plate tholeiites, while the tholeiite lies in the volcanic-arc field.

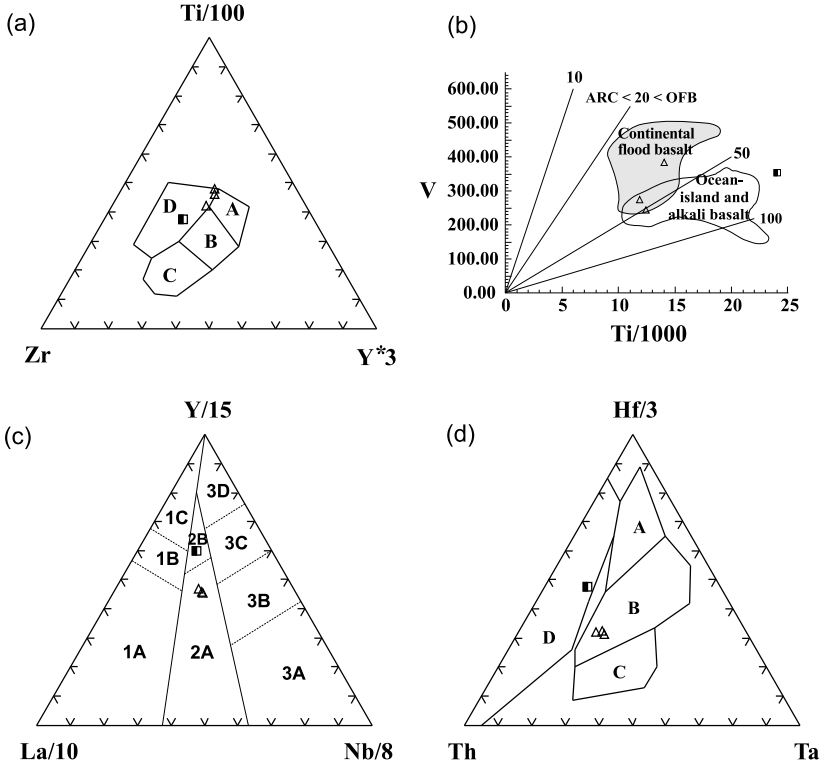

Figure 6 (a) Zr–Ti–Y diagram of Pearce & Cann (1973). A–B, low-K tholeiites; B, ocean-floor basalts; B–C, calc-alkaline basalts; D, within-plate basalts. (b) Ti–V diagram of Shervais (1982). Note that the intraplate alkaline basalts plot in the continental flood basalt field. ARC, island-arc basalts; OFB, ocean-floor basalts. (c) La–Y–Nb diagram of Cabanis & Lecolle (1989). Once again the alkali basalts overlie the continental basalt field. 1A, calc-alkali basalts; 1B, overlap between 1A and 1B; 1C, volcanic-arc tholeiites; 2A, continental basalts; 2B, backarc basalts (not well defined); 3A, alkali basalts; 3B–3C, E-MORB; 3D, N-MORB. (d) Th–Hf–Ta diagram of Wood (1980). Same fields as in Figure 4.

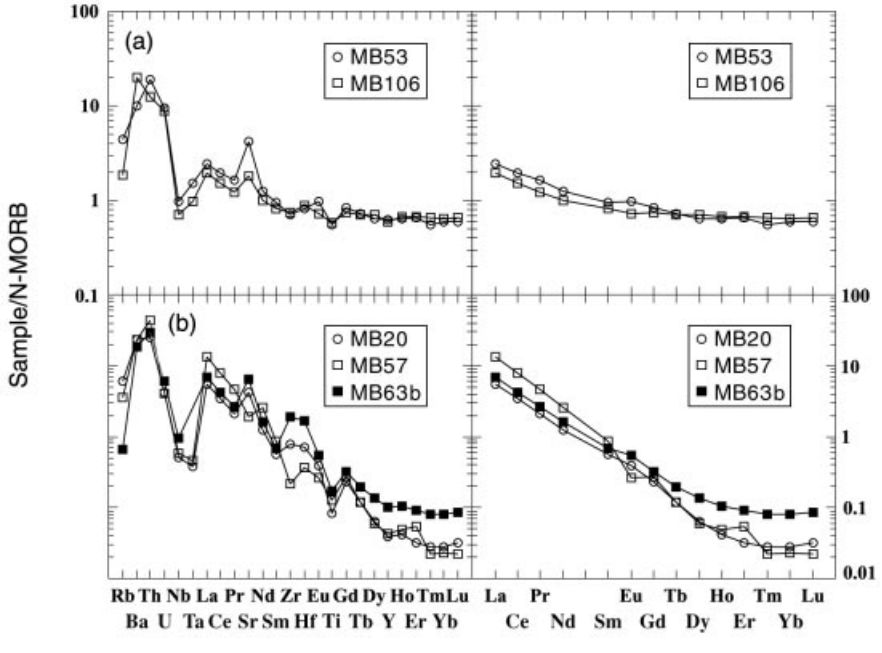

Figure 7 N-MORB-normalised incompatible multi-element (left) and REE (right) diagrams of (a) the basaltic andesites (calc-alkaline suite I) and (b) trondhjemite–tonalites (calc-alkaline suite II), from the V4 event. Note the strong arc signatures of both suites and the extremely HREE-depleted nature of the trondhjemite–tonalites.

V4 INTRUSIVE ROCKS

The intermediate lithologies from the V4 magmatic event of the Marlborough terrane are correlated with similar rocks from South Island in the Percy Isles based on lithology, geochemical trends, and the unusual occurrence of adakites common to both regions. Below we provide geochemical data for rocks of the V4 event represented in the Marlborough terrane. However, their age and geochemical significance are discussed separately (Bruce & Niu 2000).

Major elements for basaltic andesites from the Marlborough terrane are similar to the average basaltic andesites of the southwest Pacific (Ewart 1982) in Table 2. The V4 series rocks are somewhat higher in MgO and Na_2O and lower in Al_2O_3, FeO* and K_2O than the average southwest Pacific arc basaltic andesite. These differences could reflect a higher degree of partial melting (low Al_2O_3) in the V4 basaltic andesites as well as subsequent alteration

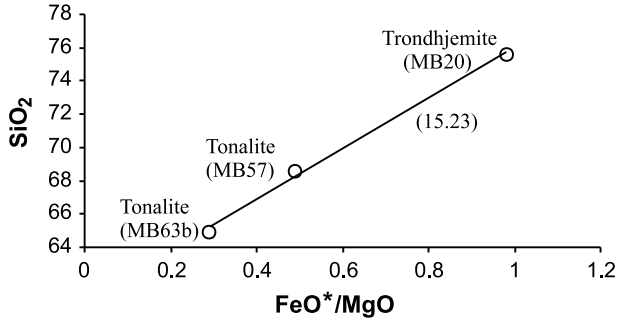

Figure 8 SiO_2 *vs* FeO*/MgO diagram denoting a strong fractionation trend for the V4 trondhjemite–tonalite suite. The bracketed number refers to the slope of the trend line, which according to the division of Miyashiro (1974), depicts the suite as calc-alkaline (Figure 2). FeO* = total iron reported as FeO.

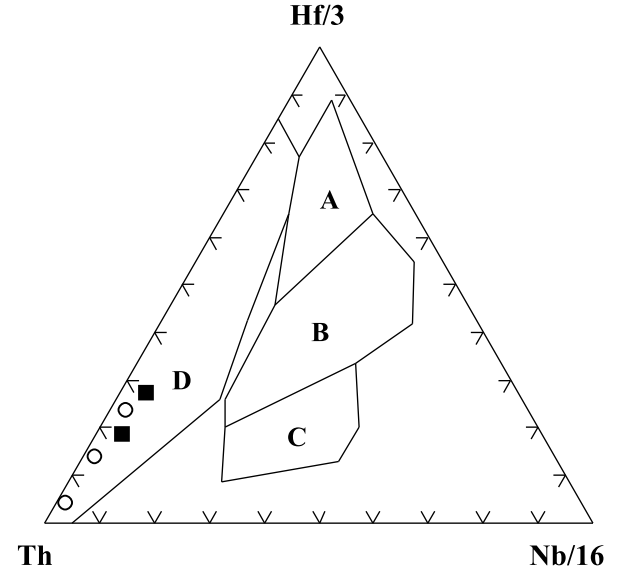

Figure 9 Th–Hf–Nb discrimination diagram of Wood (1980) for V4 magmatism. Same fields as in Figure 4. Samples plot in the volcanic-arc field with both suites having Hf/Th ratios < 3, typical of calc-alkaline magmas. ■, basaltic andesite–diorite; ○, trondhjerite–tonalite.

(high Na_2O and low K_2O). On N-MORB normalised multi-element diagrams (Figure 7) the basaltic andesites display characteristic arc signatures with enrichment in Ba, Th, Sr and the LREE [$(Sm/Nd)_{N\text{-}MORB}$ = 0.76–0.82] and depletion in Nb, Ta and Ti. These trace-element characteristics may reflect either addition of LILE and LREE to the mantle wedge from the subducted slab (Pearce 1983; McCulloch & Gamble 1991) or from the melting of slightly enriched sources of the mantle wedge in the presence of an HFSE-bearing residual phase (Morris & Hart 1983; Sun & McDonough 1989).

A further magmatic suite is defined by a trondhjemite–tonalite association from the V4 event. A linear correlation defined by SiO_2 and FeO*/MgO ratios (Figure 8) can be explained by fractionation processes. This trend also suggests that these elements have been largely unaffected by metamorphism and that they retain their original calc-alkaline signature. The trondhjemite association displays similarities with ophiolitic plagiogranite (e.g. quartz- and albite-rich), but are unusual in that they have high Al_2O_3 (≥ 15%) and extremely low heavy-REE (HREE) abundances. They are also characterised by depletions of the HFSE (Nb, Ta and Ti) and enrichments of the LILE (Ba and Sr), Th and LREE. The high Al_2O_3 (≥ 15%) and Sr (> 300 ppm), low Rb/Sr ratios (≤ 0.01) as well as low Y (< 3 ppm), Nb (< 3 ppm) and Yb (< 0.3 ppm) suggest that these rocks resemble the high-Al trondhjemite–tonalite–dacite suites of the Archaean. These suites also occur in some modern island-arc environments (adakites) probably produced by the melting of crustal lithologies of young (< 25 million years), hot subducting oceanic lithosphere (Drummond & Defant 1990; Drummond *et al.* 1996).

Both the basaltic andesite and trondhjemite suites plot in the volcanic-arc field on the Th–Hf–Nb diagram of Wood (1980) (Figure 9) and have low Hf/Th ratios (< 3), typical of calc-alkaline volcanics. The granitoids plot in the volcanic-arc granitoid field on the Nb–Y and Rb versus Nb + Y diagrams of Pearce *et al.* (1984) (Figure 10).

ISOTOPE DATING

Nd and Sm were separated from whole-rock and mineral fractions using standard column chemistry techniques and $^{147}Sm/^{144}Nd$ and $^{143}Nd/^{144}Nd$ isotopic ratios were measured on a Fisons VG 54-30 Sector multicollector mass spectrometer at the University of Queensland. Sample preparation and analytical details are provided in Bruce *et al.* (2000). Sm–Nd isotopic results are given in Table 3.

V2 intrusive rocks

The $^{147}Sm/^{144}Nd$ ratios obtained from four whole-rock basaltic dykes correlate extremely well with their $^{143}Nd/^{144}Nd$ ratios (MSWD = 0.04). Regression of the data points (Figure 11) results in a well-defined isochron with a slope equivalent to an age of 380 ± 19 Ma and an initial $^{143}Nd/^{144}Nd = 0.512562 \pm 5$ or $\epsilon_{Nd}(t) = +8.1$. This $\epsilon_{Nd}(t)$ value is very similar to those obtained from modern island arc or backarc basin rocks (DePaolo 1988) and reinforces

our interpretation of an oceanic-arc setting based on trace-element data.

V3 intrusive rocks

Sm–Nd isotopic data of whole-rock samples and one plagioclase separate for the intraplate (V3) magmatic event are shown in Figure 12. Mineral data were required because of the insufficient spread in $^{147}Sm/^{144}Nd$ ratios in whole rocks alone. Regression of the data produces a four-point isochron (MSWD = 0.67) with a slope equivalent to an age of 293 ± 35 Ma and an initial $^{143}Nd/^{144}Nd_i = 0.512611 \pm 10$ or $\epsilon_{Nd}(t) = +6.8$. This initial $\epsilon_{Nd}(t)$ value is typical of values recorded in some modern oceanic-island basalts (Zindler & Hart 1986), but is also characteristic of modern uncontaminated lavas from continental intraplate settings (+ 6 to + 8: DePaolo 1988), suggesting their derivation from a similar, slightly enriched, mantle source (Thompson *et al.* 1983, 1984; Cox & Hawkesworth 1985; DePaolo 1988).

DISCUSSION

Revealing the tectonic environments (i.e. island arc or Andean margin for the arc assemblages or oceanic or continental for the intraplate sequence) of the V2, V3 and V4 magmatic overprints is important in reconstructing the palaeotectonics of the northern New England Fold Belt.

Table 3 Sm–Nd isotopic results for whole rocks and mineral separate from V2 and V3 magmatism.

	Rock type	Sm (ppm)	Nd (ppm)	$^{147}Sm/^{144}Nd$	$^{143}Nd/^{144}Nd$	$\epsilon_{Nd}(0)$	$\epsilon_{Nd}(562)$	ϵ_{Nd}(isochron)
V2 magmatism								
MB5	Dolerite	3.46	10.24	0.2040	0.513069	+8.41	+8.06	
MB16	Dolerite	5.5	26.52	0.1254	0.512874	+4.60	+8.07	+ 8.07 ± 0.10
MB31	Dolerite	3.61	10.86	0.2012	0.513063	+8.29	+8.08	
MB55	Dolerite	2.37	8.53	0.1712	0.512989	+6.85	+8.09	
V3 magmatism							$\epsilon_{Nd}(293)$	
MB38	Dolerite	7.84	26.47	0.1791	0.512951	+6.11	+6.77	
MB59	Dolerite	4.69	17.91	0.1583	0.512917	+5.44	+6.88	+ 6.84 ± 0.19
MB62	Dolerite	4.76	17.84	0.1616	0.512922	+5.54	+6.86	
MB59-plag	Plagioclase	2.25	10.51	0.1295	0.512857	+4.27	+6.79	

Errors used in isochron calculation are true analytical errors, including sources of such errors as instrumental reproducibility. These are 0.0016% on $^{143}Nd/^{144}Nd$ ratios and 0.5% on $^{147}Sm/^{144}Nd$ ratios.

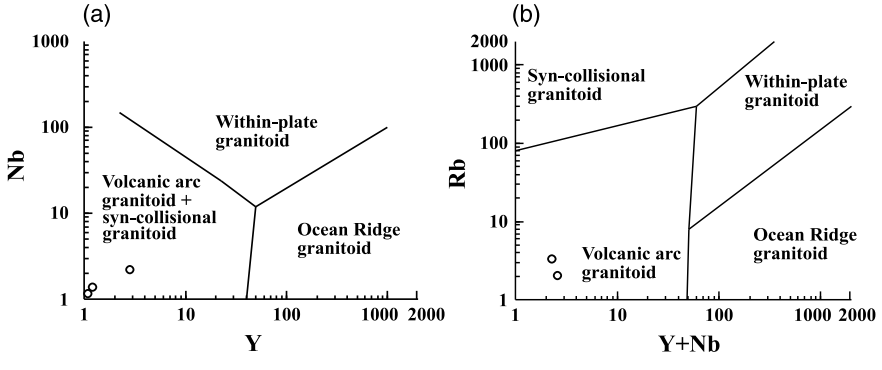

Figure 10 Nb *vs* Y and Rb *vs* Y + Nb diagrams of Pearce *et al.* (1984). Note that the V4 trondhjemite–tonalites fall in the volcanic-arc granitoid field.

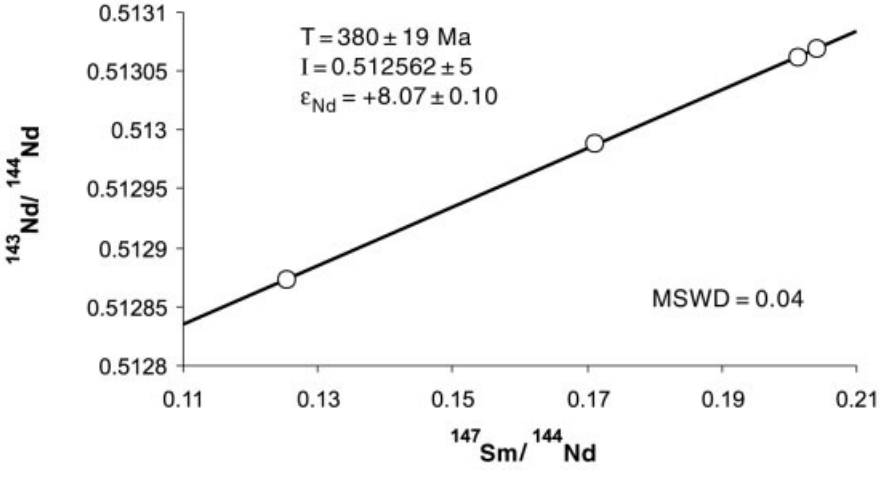

Figure 11 Sm–Nd isochron diagram constructed for rocks of V2 magmatism. T, age of isochron; I, initial $^{143}Nd/^{144}Nd$; ϵ_{Nd}, initial epsilon Nd value. All reported errors are at 2σ. Note that the symbol size used is larger than the error bars for each sample. MSWD = 0.04.

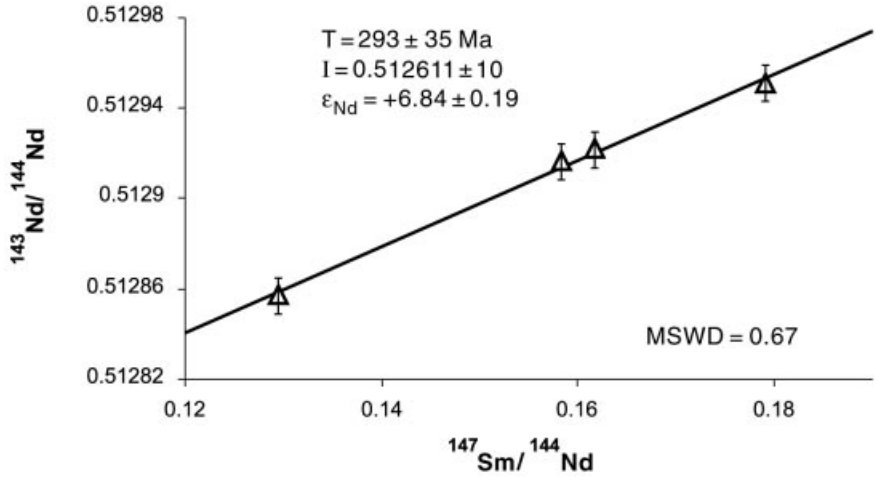

Figure 12 Sm–Nd isochron diagram constructed for rocks of V3 magmatism. T, I and ϵ_{Nd} as in Figure 11. All reported errors are at 2σ. Note that samples include vertical error bars. Horizontal error bars are smaller than the symbol size. MSWD = 0.67.

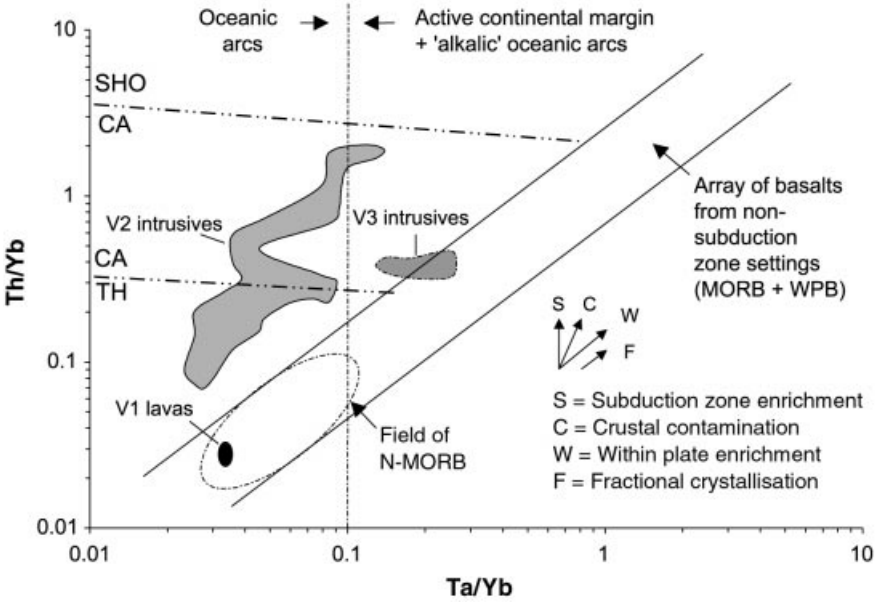

Figure 13 Th/Yb *vs* Ta/Yb after Pearce (1983). Note that rocks from the V2 event plot in the oceanic-arc field whereas there is overlap between within-plate basalts and continental-arc fields for V3 magmatism. V1 lavas from the Marlborough ophiolite (Bruce *et al*. 2000, this issue) plot in the field of N-type MORB. SHO, Shoshinite; CA, Calc alkaline; TH, tholeiite.

This is particularly true for the V2 event, which has a mid-Devonian age. This age corresponds to volcanism in the Mt Morgan Assemblage of the former Calliope terrane, a unit which unconformably underlies the Yarrol terrane (Figure 1), whose origin in an island-arc or continental-margin setting is debatable (Day *et al*. 1978; Morand 1993a, b). Given the age similarity, the nature of magmatism from the V2 event may have important implications for the tectonic environment of the Mt Morgan Assemblage, which was assigned to an extensional-arc setting by Messenger (1996).

The absence of intermediate or felsic lithologies in the V2 event suggests absence of continental crustal material in the source. V2 magmatism may, therefore, have taken place in an oceanic-arc setting. The dominance of basaltic tholeiite favours such an interpretation. The occurrence of calc-alkaline basalt may reflect crustal thickening (maturing) of the arc (Miyashiro 1974). The overall incompatible-element characteristics of the V2 basaltic rocks are also consistent with an island-arc origin (Figure 3). Lithologies of V2 magmatism plot within the oceanic-arc field on the Th/Yb versus Ta/Yb diagram of Pearce (1983) (Figure 13). Radiogenic isotopes support a depleted mantle source and lack evidence for any crustal component. Depleted Nd isotopes record values similar to those obtained from modern oceanic arcs. These data suggest that an arc developed on juvenile oceanic crust in which the Mt Morgan Assemblage may have evolved behind in a backarc basin (Messenger 1996).

Tectonic discrimination diagrams (such as those used in this study) quite often result in equivocal allocations (Rollinson 1993) or the 'pigeonhole effect'. This is the case with the intraplate V3 basalts, which plot as continental basalts on some discrimination diagrams and as E-MORB and volcanic-arc basalts on others (Figure 6). This is also demonstrated in the Th/Yb versus Ta/Yb diagram where the data overlap the field of within-plate basalts and continental-arc basalts (Figure 13). However, the reason for this may be purely geological as seen, for example, in continental flood basalts, which may erupt in a variety of within-plate tectonic settings. In this case, radiogenic isotopes are also equivocal as they record $^{143}Nd/^{144}Nd$ ratios similar to both ocean-island basalt and uncontaminated lavas from some modern continental intraplate environments. Thus,

geochemistry alone cannot resolve the tectonic setting of these rocks. It is therefore useful and necessary to consider the tectonic history of the New England Fold Belt during the Late Carboniferous to Early Permian, which was a period of major extension throughout eastern Australia (Holcombe *et al*. 1997; Allen *et al*. 1998). Therefore, a continental intraplate origin for the basalts is preferred.

As we envisage that V2 magmatism took place in an oceanic island arc, the ophiolitic substrate (V1 event) could not have accreted to the Australian margin by this time. However, the nature of the V3 magmatic event suggests that the complex was part of the Australian continent by 295 Ma. Thus cratonisation must have occurred between *ca* 380 and *ca* 295 Ma.

ACKNOWLEDGEMENTS

This research was carried out as part of MCB's PhD thesis under the tenureship of an ARC research grant to Yaoling Niu and Rodney Holcombe. The authors would like to thank Marcel Regelous and Ken Collerson for assistance with Sm–Nd isotope analyses, Allan Greig for conducting some of the trace-element analyses and Sharyn Price for analysing major elements. Critical and constructive comments by journal reviewers Cecil Murray and Peter Cawood were very helpful in improving the overall quality of the paper.

REFERENCES

Allen C. M., Williams I. S., Stephens C. J. & Fielding C. R. 1998. Granite genesis and basin formation in an extensional setting: the magmatic history of the northernmost New England Orogen. *Australian Journal of Earth Sciences* **45**, 875–888.

Bruce M. C. & Niu Y. 2000. Early Permian supra-subduction zone assemblage of the South Island terrane, Percy Isles, New England Fold Belt, Queensland. *Australian Journal of Earth Sciences* **47**, 1077–1085.

Bruce M. C., Niu Y., Harbort T. A. & Holcombe R. J. 2000. Petrological, geochemical and geochronological evidence for a Neoproterozoic ocean basin recorded in the Marlborough terrane of the northern New England Fold Belt. *Australian Journal of Earth Sciences* **47**, 1053–1064.

Cabanis B. & Lecolle M. 1989. Le diagramme La/10-Y/15-Nb/8: an outil pour la discrimination des series volcaniques et la mise en evidence des processus de melange et/ou de contamination crustale. *Comptes Rendus de l'Academie des Sciences Series II* **309**, 2023–2029.

Campbell I. H., Lesher C. M., Coad P., Franklin J. M., Gorton M. P. & Thurston P. C. 1984. Rare earth element mobility in alteration pipes below massive sulfide deposits. *Chemical Geology* **45**, 181–202.

Cann J. R. 1969. Spilites from the Carlsberg Ridge, Indian Ocean. *Journal of Petrology* **10**, 1–19.

Cawood P. A. & Leitch E. C. 1985. Accretion and dispersal tectonics of the southern New England Fold Belt, eastern Australia. *In:* Howell D. G. ed. *Tectonostratigraphic Terranes of the Circum-Pacific Region,* Vol. 1. pp. 481–492. Circum-Pacific Council for Energy and Mineral Resources, Earth Science Series, Houston.

Coney P. J., Edwards A., Hine R., Morrison F. & Windrum D. 1990. The regional tectonics of the Tasman orogenic system, eastern Australia. *Journal of Structural Geology* **12**, 519–543.

Cox K. G. & Hawkesworth C. J. 1985. Geochemical stratigraphy of the Deccan Traps, at Mahabaleshwar, western Ghats, India, with implications for open system magmatic processes. *Journal of Petrology* **26**, 355–377.

Day R. W., Murray C. G. & Whitaker W. G. 1978. The eastern part of the Tasman Orogenic Zone. *Tectonophysics* **48**, 327–364.

DePaolo D. J. 1988. *Neodynium Isotope Geochemistry: an Introduction*. Springer-Verlag, Berlin.

Dick H. J. B. & Bullen T. 1984. Chromium spinel as a petrogenetic indicator in abyssal and alpine-type peridotites and spatially associated lavas. *Contributions to Mineralogy and Petrology* **86**, 54–76.

Drummond M. S. & Defant M. J. 1990. A model for trondhjemite–tonalite–dacite genesis and crustal growth via slab melting: Archean to modern comparisons. *Journal of Geophysical Research* **95**, 21 503–21 521.

Drummond M. S., Defant M. J. & Kepezhinskas P. K. 1996. Petrogenesis of slab-derived trondhjemite–tonalite–dacite/adakite magmas. *Transactions of the Royal Society of Edinburgh: Earth Sciences* **87**, 205–215.

Ewart A. 1982. The mineralogy and petrology of Tertiary–Recent orogenic volcanic rocks: with special reference to the andesitic-basaltic compositional range. *In:* Thorpe R. S. ed. *Andesites: Orogenic Andesites and Related Rocks*, pp. 25–95. John Wiley and Sons, London.

Ewart A., Brothers R. N. & Mateen A. 1977. An outline of the geology and geochemistry, and the possible petrogenetic evolution of the volcanic rocks of the Tonga–Kermadec–New Zealand island arc. *Journal of Volcanology and Geothermal Research* **2**, 205–250.

Flood P. G. 1988. New England Orogen: geosyncline, mobile belt and terranes. *In*: Kleeman J. D. ed. *New England Orogen, Tectonics and Metallogenesis*, pp. 1–6. University of New England, Armidale.

Henderson R. A., Fergusson C. L., Leitch E. C., Morand V. J., Rheinhardt J. J. & Carr P. F. 1993. Tectonics of the northern New England Fold Belt. *In:* Flood P. G. & Aitchison J. C. eds. *New England Orogen, Eastern Australia*, pp. 505–515. NEO'93 Conference Proceedings, Department of Geology and Geophysics, University of New England, Armidale.

Holcombe R. J., Stephens C. J., Fielding C. R. *et al*. 1997. Tectonic evolution of the northern New England Fold Belt: Carboniferous to Early Permian transition from active accretion to extension. *In:* Ashley P. M. & Flood P. G. eds. *Tectonics and Metallogenesis of the New England Orogen*, pp. 66–79. *Geological Society of Australia Special Publication* **19**.

Humphris S. E. 1984. The mobility of the rare earth elements in the crust. *In:* Henderson P. ed. *Rare Earth Element Geochemistry*, pp. 317–342. Elsevier, New York.

Jochum K. P. & Verma S. P. 1996. Extreme enrichment of Sb, Tl and other trace elements in altered MORB. *Chemical Geology* **130**, 289–299.

Kwiecien W. 1990. *Silicate Rock Analysis by AAS*. School of Geology, Queensland University of Technology, Brisbane.

Leitch E. C. 1974. The geological development of the southern part of the New England Fold Belt. *Journal of the Geological Society of Australia* **21**, 133–156.

Leitch E. C. 1975. Plate tectonic interpretation of the Palaeozoic history of the New England Fold Belt. *Geological Society of America Bulletin* **86**, 141–144.

McCulloch M. T. & Gamble J. A. 1991. Geochemical and geodynamical constraints on subduction zone magmatism. *Earth and Planetary Science Letters* **102**, 358–374.

Messenger P. R. 1996. Relationships between Devonian magmatism and Au–Cu mineralisation at Mt Morgan, central Queensland. PhD thesis, University of Queensland, Brisbane (unpubl.).

Miyashiro A. 1974. Volcanic rock series in island arcs and active continental margins. *American Journal of Science* **274**, 321–355.

Morand V. J. 1993a. Stratigraphy and tectonic setting of the Calliope Volcanic Assemblage, Rockhampton area, Queensland. *Australian Journal of Earth Sciences* **40**, 15–30.

Morand V. J. 1993b. Structure and metamorphism of the Calliope Volcanic Assemblage: implications for Middle to Late Devonian orogeny in the northern New England Fold Belt. *Australian Journal of Earth Sciences* **40**, 257–270.

Morris J. D. & Hart S. R. 1983. Isotopic and incompatible trace element constraints on the genesis of island arc volcanics from Cold Bay and Amak Island, Aleutians, and implications for mantle structure. *Geochimica et Cosmochimica Acta* **47**, 2015–2030.

Murray C. G. 1974. Alpine-type ultramafics in the northern part of the Tasman Geosyncline—possible remnants of Palaeozoic ocean floor. *In*: Denmead A. K., Tweedale G. W. & Wilson A. F. eds. *The Tasman Geosyncline—a Symposium*, pp. 161–181. Geological Society of Australia, Queensland Division, Brisbane.

MURRAY C. G., FERGUSSON C. L., FLOOD P. G., WHITAKER W. & KORSCH R. J. 1987. Plate tectonic model interpretation for the Carboniferous evolution of the New England Fold Belt. *Australian Journal of Earth Sciences* **34**, 213–236.

NIU Y. & HÉKINIAN R. 1997. Basaltic liquids and harzburgitic residues in the Garrett Transform: a case study at fast-spreading ridges. *Earth and Planetary Science Letters* **146**, 243–258.

PEARCE J. A. 1976. Statistical analysis of major element patterns in basalts. *Journal of Petrology* **17**, 15–43.

PEARCE J. A. 1982. Trace element characteristics of lavas from destructive plate boundaries. *In:* Thorpe R. S. ed. *Andesites: Orogenic Andesites and Related Rocks*, pp. 525–548. John Wiley and Sons, London.

PEARCE J. A. 1983. Role of the sub-continental lithosphere in magma genesis at active continental margins. *In:* Hawkesworth C. J. & Norry M. J. eds. *Continental Basalts and Mantle Xenoliths*, pp. 230–249. Shiva, Nantwich.

PEARCE J. A. & CANN J. R. 1973. Tectonic setting of basic volcanics determined using trace element analyses. *Earth and Planetary Science Letters* **19**, 290–300.

PEARCE J. A., HARRIS N. B. W. & TINDLE A. G. 1984. Trace element discrimination diagrams for the tectonic interpretation of granitic rocks. *Journal of Petrology* **25**, 956–983.

PERFIT M. R., GUST D. A., BENCE A. E., ARCULUS R. J. & TAYLOR S. R. 1980. Chemical characteristics of island arc basalts: implications of mantle sources. *In:* Le Maitre R. W. & Cundari A. eds. *Chemical Characterisation of Tectonic Provinces*, pp. 227–256. Chemical Geology **30**.

ROLLINSON H. R. 1993. *Using Geochemical Data: Evaluation, Presentation, Interpretation*. Longman Scientific and Technical, New York.

SAUNDERS A. D. & TARNEY J. 1979. The geochemistry of basalts from a back-arc spreading centre in the East Scotia Sea. *Geochimica et Cosmochimica Acta* **43**, 555–572.

SHERVAIS J. W. 1982. Ti–V plots and the petrogenesis of modern and ophiolitic lavas. *Earth and Planetary Science Letters* **59**, 101–118.

SUN S-S. & MCDONOUGH W. F. 1989. Chemical and isotopic systematics of oceanic basalts: implications for mantle composition and processes. *In:* Saunders A. D. & Norry M. J. eds. *Magmatism in Ocean Basins*, pp. 313–345. Geological Society of London Special Publication **42**.

THOMPSON R. N., MORRISON M. A., DICKEN A. P. & HENDRY G. L. 1983. Continental flood basalts . . . arachnids rule OK? *In:* Hawkesworth C. J. & Norry M. J. eds. *Continental Basalts and Mantle Xenoliths*, pp. 158–185. Shiva, Nantwich.

THOMPSON R. N., MORRISON M. A., HENDRY G. L. & PARRY S. J. 1984. An assessment of the relative roles of a crust and mantle in magma genesis: an elemental approach. *Philosophical Transactions of the Royal Society of London* **A310**, 549–590.

WOOD D. A. 1980. The application of a Th–Hf–Ta diagram to problems for tectonomagmatic classification and to establishing the nature of crustal contamination of basaltic lavas of the British Tertiary volcanic province. *Earth and Planetary Science Letters* **50**, 11–30.

ZINDLER A. & HART S. 1986. Chemical geodynamics. *Annual Review of Earth and Planetary Science* **14**, 493–571.

Received 1 November 1999; accepted 17 July 2000

APPENDIX 1: SAMPLE LOCATIONS

Sample	AMG coordinates	Sample	AMG coordinates
MB5	200815E; 7463633N	MB55	793194E; 7465856N
MB16	200225E; 7464210N	MB57	799710E; 7465616N
MB20	798555E; 7458320N	MB59	799269E; 7464653N
MB31	200991E; 7462075N	MB62	799247E; 7464595N
MB38	804382E; 7455767N	MB96	797150E; 7479503N
MB53	793928E; 7465446N	MB112	199183E; 7466169N

Marlborough (8852) and Princhester (8952) 1:100 000 sheets.